SAND2011-6623C

Analyzing the Effect of Large Pressure Changes on the Stability of Large-Diameter Caverns for the Strategic Petroleum Reserve Using the Multi-Mechanism Deformation Model

S.R. Sobolik & B.L. Ehgartner
Sandia National Laboratories, Albuquerque, New Mexico, USA

ABSTRACT: This report presents a case study of how computational analyses may be used in conjunction with site data to advise site operations responding to a wellbore casing failure. The analyses performed in this report were in response to a borehole casing failure discovered at the U.S. Strategic Petroleum Reserve's West Hackberry site. The intent of these calculations is to utilize high-performance geomechanical analyses to provide real-time support to field operations and assure cavern integrity. Additional analyses in this report demonstrate the capability to anticipate potential problems that may occur in the field, and plan operational procedures to prevent or mitigate negative consequences.

1 INTRODUCTION

The U.S. Strategic Petroleum Reserve (SPR), operated by the U.S Department of Energy (DOE), stores crude oil in 62 caverns located at four different sites in Texas (Bryan Mound and Big Hill) and Louisiana (Bayou Choctaw and West Hackberry). The petroleum is stored in solution-mined caverns in salt dome formations. West Hackberry is located in the extreme southwestern corner of Louisiana, some 24 km from the Louisiana/Texas border to the west and the Gulf of Mexico to the south (Munson, 2006). The geological characteristics related to the West Hackberry site were first described by Whiting (1980). The updated three-dimensional models of Rautman et al. (2004) used a more refined analysis of the data and produced models of the dome that differed slightly from the earlier models. The West Hackberry dome consists of the more-or-less typical geologic sequence of rocks. With increasing depth below the ground surface, initially there is roughly 480 m of soil and unconsolidated gravel, sand, and mud, followed by approximately 120 m of caprock, consisting of anhydrite and carbonate (a conversion product of anhydrite). Generally, the upper portions of the caprock consist of the anhydrite conversion products of gypsum and dolomite, while the lower portion of the caprock is the initial anhydrite residue from the solution of the original domal material. The caprock is generally lens shaped with the thickest part of the lens over the central portion of the dome, tapering to thin edges toward the periphery of the dome.

At the West Hackberry site, the five caverns known as Phase 1 – Caverns 6, 7, 8, 9, and 11 – were created as early as 1946 and were used for brining and brine storage before the SPR took ownership of them in 1981. After that time, seventeen other storage caverns (numbered 101 to 117) were created over an eight-year period. The post-1981 caverns were built via solution mining, and all have a generally cylindrical shape (more specifically, frustums with the larger diameter at the top) of approximately 600 m (2000 feet) height and 30-45 m (100-150 feet) in radius. The Phase 1 caverns, however, were originally built for brine production, and thus they were constructed with less concern about the long-term stability of the cavern shape. Cavern 6 at the West Hackberry site has an unusual dish-like shape with a large rim around the circumference. It is also in close proximity to Cavern 9, an hourglass-shaped cavern. A profile view of Cavern 6 is shown in Figure 1, and a representation of Caverns 6 and 9 drawn in their full volume and proximity is shown in Figure 2. High-resolution sonar measurements performed on Cavern 6 in 1980 are listed in Table 1 along with the average and maximum ceiling spans. The sonars of Cavern 6, taken from the three different Cavern 6 wells, are in close agreement and show that the ceiling of Cavern 9 is located 70 m (230 feet) from its edge. The closest point of approach is with the lower lobe of Cavern 9, at approximately 60 m (200 feet).

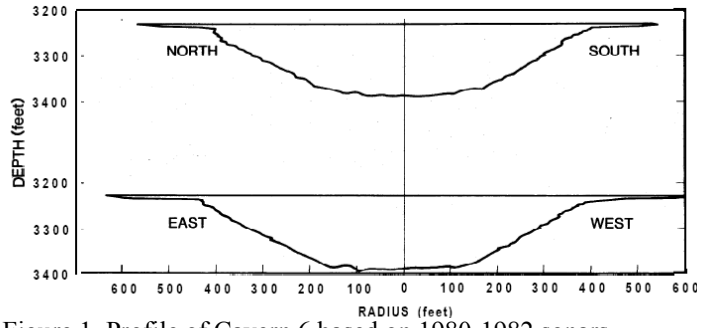

Figure 1. Profile of Cavern 6 based on 1980-1982 sonars.

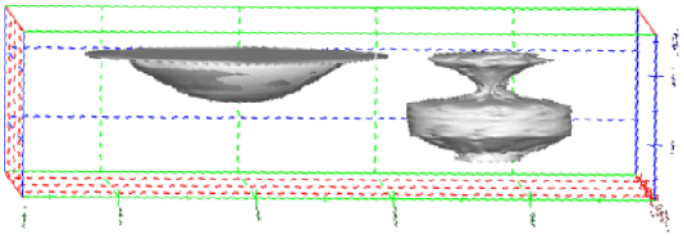
Figure 2. Caverns 6 (left) and 9 (right), from the most recent (1982) sonar and strapping data.

Table 1. Cavern shape case summary.

	Well	Avg. Ceiling Span, m (ft)	Maximum Ceiling Span, m (ft)
5/21/1980	6	353.0 (1158)	378.9 (1243)
5/21/1981	6	349.0 (1145)	375.2 (1231)
3/21/1980	6c	342.6 (1124)	369.4 (1212)
3/21/1980	6b	344.1 (1129)	361.8 (1187)

Mechanical analyses of the West Hackberry site were recently published (Sobolik and Ehgartner, 2009), and they indicate that the dish-like shape of Cavern 6 make it prone to significant subsidence during normal operations, and may potentially be at risk of dilatant and tensile damage around the cavern perimeter during repressurization after a workover. The analyses in Sobolik and Ehgartner (2009) modeled the salt's creep behavior with the power law creep model along with a reduced elastic modulus. While this approach gives good results of long-term behavior, it probably overestimates the mechanical reaction of the salt to changes in pressure over a short time interval. Recently, Sandia improved its implementation of the M-D multi-mechanism deformation (M-D) model (Sobolik et al. 2010), which is a rigorous mathematical description of both transient and steady-state creep phenomena. The M-D model provides a more realistic model of the transient behavior of salt under pressure change conditions such as a workover.

Recent problems with the integrity of Well 6 led to a workover of the cavern. Because of concerns of potential tensile cracking around the perimeter of Cavern 6 upon repressurization, several new sets of calculations were performed on West Hackberry utilizing the M-D model. The calculations modeling the workover of Cavern 6 resulted in operational guidance to the SPR that permitted increasing the pressure quickly to an intermediate value to minimize storage loss, and then slowly increasing the pressure to a maximum operating pressure. Additional calculations were performed to simulate a workover in Cavern 9 three months after the completion of the Cavern 6 procedure, and to simulate the effect of operating Caverns 6 and 9 as a gallery.

2 DESCRIPTION OF EVENT AT WEST HACKBERRY CAVERN 6

Prior to the events of September 2010, Cavern 6 had three cemented and cased wells, two of which also had liners due to earlier well failures. The most recent well failure occurred in the remaining unlined Well 6. The 7-inch (178-mm) production casing was logged using a Multi-Sensor Caliper as part of an ongoing program to determine the condition of SPR wellbores. The caliper survey run on August 23, 2010 and confirming camera images taken on September 1, 2010 provided compelling evidence of parted casing and severe deformation within the Well 6 cased wellbore, particularly at depths of approximately 59 and 777 meters (195 and 2,550 feet subsurface). Figure 3 shows some images of the damaged wellbore. The damage is a result of tensile strains generated along the axis of the wellbore due to cavern creep and subsidence.

The decision was made to plug and abandon the damaged well. The process required an extended workover period. The wellhead pressure was reduced to atmospheric starting on September 28, 2010, and cementing the wellbore to the Bradenhead Flange was not achieved until January 5, 2011.

Figure 3. Camera shots showing parted casing (upper- looking down well, lower- sidewall image) just above collar at 60.8 m (199.5 feet) (courtesy DM Petroleum Operations Co.).

3 RESULTS OF EARLIER ANALYSES

An earlier set of analyses was performed of the mechanical behavior of the caverns at the West Hackberry site (Sobolik and Ehgartner, 2009). These analyses indicated several concerns about Caverns 6 and 9:

- Because of the dish-like shape of Cavern 6, the perimeter of the cavern is at risk of dilatant and tensile damage, particularly at the end of a workover operation.
- Because of expected tensile cracking potential near Cavern 6, the close proximity of Cavern 9 (60 meters at their closest point) poses a risk of inter-cavern communications. The potential exists for a crack to propagate from Cavern 6 and intersect Cavern 9, causing cavern pressures to equilibrate. An operational scenario of having Cavern 9 in workover mode during the breach would pose a serious risk to operational safety and containment of oil. A breach when Cavern 6 is fully repressurized (the most likely condition) could abruptly pressurize Cavern 9 and potentially result in oil loss in the absence of a wellhead or if the blowout preventer faulted. This could pose a safety risk to the workover crew and potential environmental damage.
- Cavern 9 has a middle section with a smaller radius, giving a cross-section of the cavern the look of a bell with a mid-cavern ledge. This ledge and the cavern wall underneath supporting the ledge are also locations with a significant potential for dilatant damage during workover operations.
- Workovers performed on Cavern 9 wells should be performed no sooner than one year after the completion of a workover in Cavern 6. This period will allow the stressed salt around Cavern 6 enough time to heal and attain near-hydrostatic stress values, so to minimize the possibility of cracking the salt between Caverns 6 and 9. Performing the workovers in the opposite order (Cavern 9, then Cavern 6) does not appear to need such a stringent requirement, although it may be prudent to keep the same delay.

Because of the results of these previous analyses, the SPR site office was already sensitive to the potential integrity issues regarding Cavern 6. Therefore, in response to the decision by the SPR site office to initiate a workover on Cavern 6, a new set of calculations was performed to develop recommedations for the repressurization of the cavern. These analyses were performed with the same computational mesh, boundary conditions, and cavern operating conditions as the Sobolik and Ehgartner (2009) analyses, but with greater detail given to the rate of repressurization, and with an improved material model for the salt.

4 DESCRIPTION OF THE MODEL

This analysis utilized JAS3D, Version 2.0.F (Blanford et al., 2001), a three-dimensional finite element program developed by Sandia National Laboratories, and designed to solve large quasi-static nonlinear mechanics problems. Several constitutive material models are incorporated into the program, including models that account for elasticity, viscoelasticity, several types of hardening plasticity, strain rate dependent behavior, damage, internal state variables, deviatoric creep, and incompressibility. The continuum mechanics modeled by JAS3D are based on two fundamental governing equations. The kinematics are based on the conservation of momentum equation, which can be solved either for quasi-static or dynamic conditions (a quasi-static procedure was used for these analyses). The stress-strain relationships are posed in terms of the conventional Cauchy stress.

Historically, three-dimensional geomechanical simulations of the behavior of the caverns at SPR facilities have been performed using a power law creep model, which evaluates only the secondary steady-state salt creep mechanism. Because the transient creep mechanism is not represented in this model, the common practice has been to use a reduction factor for the elastic modulus. Using this method, and calibrating the creep coefficient to field data such as cavern closure and surface subsidence, analysis agreement with observed phenomena has ranged from adequate to very good, depending upon the degree of homogeneity at a particular site. However, the power law creep model used in this manner is not well suited for modeling short-term events such as pressure changes due to a workover. The artificially low elastic modulus causes an overestimation of the deformation response to depressurization and repressurization, and also incorrectly models the stress equilibration response of the salt after such an event.

Recently, enhancements have been completed to the integration algorithm within the model to create a more stable implementation of the multi-mechanism deformation (M-D) model (Sobolik et al., 2010). The M-D model is a rigorous mathematical description of both transient and steady-state creep phenomena. It was originally developed by Munson and Dawson (1979, 1982, and 1984) and later extended by Munson et al. (1989). This constitutive model considers three well-recognized fundamental features of a creeping material: a steady-state creep rate, a transient strain limit, and both a work-hardening and recovery time rate of change (*i.e.,* curvature). Because of the highly non-linear

nature of the curvature of the transient strain response, this model has been difficult to integrate in a fully three-dimensional calculation for a model with hundreds of thousands of elements. Many published papers exist presenting two-dimensional calculations using the M-D model, but three-dimensional, large-scale simulations have been more difficult due to the model's high nonlinearity. Full descriptions of the M-D model and the integration algorithm enhancements are provided in Sobolik et al. (2010).

The computational domain developed for Sobolik and Ehgartner (2009) for the West Hackberry cavern field encompasses the eastern half of the salt dome, with a vertical symmetry plane through six WH caverns (110, 109, 103, 101, 105, and 117). The mesh for the computational model is illustrated in Figures 4 and 5. Figure 4 shows the entire mesh used for these calculations, and Figure 5 shows the same view with the overburden and caprock removed to expose the salt formation. Four material blocks were used in the model to describe the stratigraphy: the overburden, caprock, salt dome and sandstone surrounding the salt dome. The overburden is made of sand, and the caprock layer is made of gypsum or limestone. Figure 6 shows two views of the layout of the meshed caverns used for these calculations, which includes the six half caverns listed above, which are spaced approximately 230 m (750 feet) center-to-center, plus full cavern representations for 108 and the Phase 1 caverns (6, 7, 8, 9, and 11).

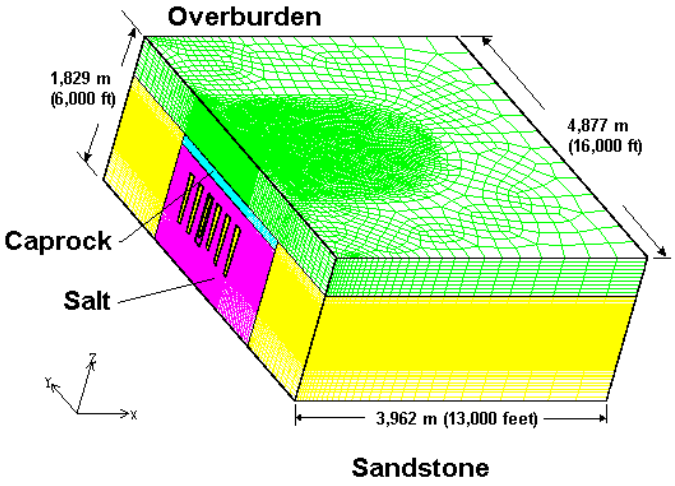

Figure 4. Computational mesh used for the West Hackberry calculations.

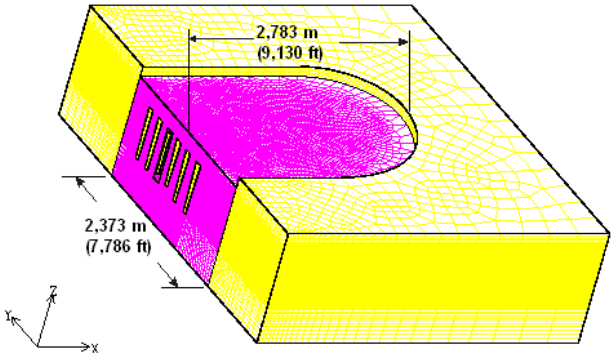

Figure 5. Computational mesh showing the salt formation and surrounding sandstone.

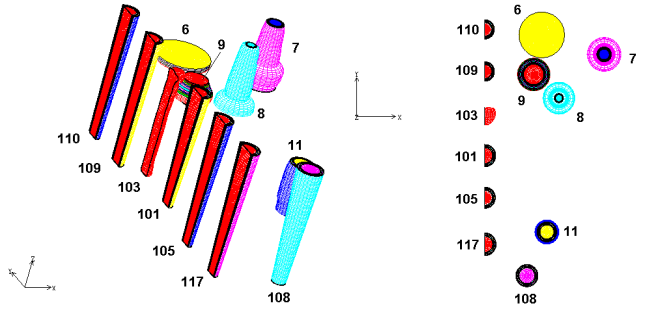

Figure 6. West Hackberry caverns included in the computational mesh (two views).

5 DESCRIPTION OF THE ANALYSIS OF A WORKOVER ON CAVERN 6

The 1980 sonar data from Cavern 6 indicate that the approximately 60-m (200-feet) wide "rim" encircling the cavern has been present since at least 1980, and was about 10 feet thick at the edge of the dish or bowl portion of the cavern. Unfortunately, the 1981 sonar measurements are the last data taken of the cavern profile. The current condition of the rim of Cavern 6 is not known. This may be important for two reasons. One, the extension of the flat wide volume of the cavern may increase the already-high fracture potential around the perimeter, and consequently cause the cavern ceiling to subside more. Two, because of the geometry of the cavern, it is possible that the rim has been pinched off from the rest of the cavern, potentially trapping oil in the pinched section or in pockets near the rim that are at higher elevations than the access holes in the cavern ceiling. Therefore, there are three probable current conditions of the rim around Cavern 6:

- The rim is highly compressed, but there is still enough oil in it to allow pressure communication from the main cavern out to the edge of the rim; or
- The rim is completely pinched off at the edge of the main part of the cavern, meaning there is in essence no more rim; or
- The rim is pinched off somewhere between the main cavern and the original rim edge.

Mechanical simulations were performed with JAS3D and the M-D model assuming either communication with the edge of the rim, or that the rim no longer exists. The analyses were identical to those performed for Sobolik and Ehgartner (2009), except that the M-D model was used instead of the power law creep model, and the pressure changes during the workover period for Cavern 6 were altered. For all the analyses, the wellhead pressure in Cavern 6 was dropped from its normal operating pressure of 6.2 MPa (900 psi) to 0 MPa for the workover in 120 hours (5 days), and then held at 0

MPa for an additional 55 days before repressurization. The parameters used for the M-D model are listed in Table 2. The properties were developed from Munson (1998), with a multiplier of 1.2 added to K_0 to better match subsidence and cavern closure data from West Hackberry. Five sets of calculations were performed:

- Cavern with rim, raise wellhead pressure from 0 to 6.2 MPa (900 psi) in 24 hours (1 day).
- Cavern with rim, raise wellhead pressure from 0 to 6.2 MPa (900 psi) in 72 hours (3 days).
- Cavern with rim, raise wellhead pressure from 0 to 6.2 MPa (900 psi) in 120 hours (5 days).
- Cavern with a closed rim, raise wellhead pressure from 0 to 6.2 MPa (900 psi) in 72 hours (3 days).
- Cavern with rim, with a staged repressurization: raise wellhead pressure from 0 to 4.8 MPa (700 psi) in 72 hours (3 days), followed by a seven-day period raising the pressure to 5.9 MPa (850 psi).

Table 2. M-D Model mechanical properties used for West Hackberry salt.

Property	West Hackberry, soft salt properties
Density, kg/m^3	2300 (144 lb/ft^3)
Elastic modulus, GPa	31.0 (4.50 ×10^6 psi)
Shear modulus G, GPa	12.4 (1.80 ×10^6 psi)
Poisson's ratio	0.25
Primary Creep Constant A_1, sec^{-1}	9.81 ×10^{22}
Exponent n_1	5.5
Q_1, cal/mol	25000
Secondary Creep Constant A_2, sec^{-1}	1.13 ×10^{13}
Exponent n_2	5.0
Q_2, cal/mol	10000
B_1, sec^{-1}	7.121×10^6
B_2, sec^{-1}	3.55×10^{-2}
σ_0, MPa	20.57 (2983 psi)
q	5335
m	3.0
K_0	7.53×10^5
c	0.009198
α	-17.37
β	-7.738
δ	0.58

Figure 7 shows the maximum stress around the perimeter of the cavern during repressurization. For the simulations that assume communication with the edge of the rim still exists, the maximum stress is at the edge of the rim; for the case with a closed rim, the stress occurs at the perimeter of the main bowl of the cavern. The "x" on each curve indicates when each simulation reaches 4.8 MPa (700 psi) wellhead pressure. Note that for the three cases with a rim and a steady repressurization, the maximum stress become tensile when the wellhead pressure reaches its maximum simulation pressure of 6.2 MPa. Note also that there is some improvement as the repressurization period increases. For the case with a closed rim, the maximum stress nears but does not become tensile at its maximum wellhead pressure. This result is significant, because the corresponding results using the power law creep model in Sobolik and Ehgartner (2009) indicated that tensile stresses would occur during this process; the M-D model, which handles transient stress effects more realistically, shows that tension should not occur, although the predicted stresses come uncomfortably close to tension. For the case of the staged repressurization, the maximum stress reaches its maximum value of 2.1 MPa in compression at 10 days and 5.9 MPa wellhead pressure, and then begins to re-equilibrate to in situ stress. These results indicate that the best approach for repressurization is to relatively quickly (i.e., in 3 days) increase the wellhead pressure to 4.8 MPa to mitigate further storage capacity loss, then take a much longer time (at least seven days) to increase the wellhead pressure to the minimum of the normal operating range or 5.9 MPa. Figure 8 shows the resulting stress re-equilibration for up to 450 days after the end of the workover. Note that the maximum stress has not reached the in situ value before the end of the analysis at 450 days. Because of the proximity of Cavern 9, this result would seem to reinforce the recommendation to wait at least one year between workovers of Caverns 6 and 9.

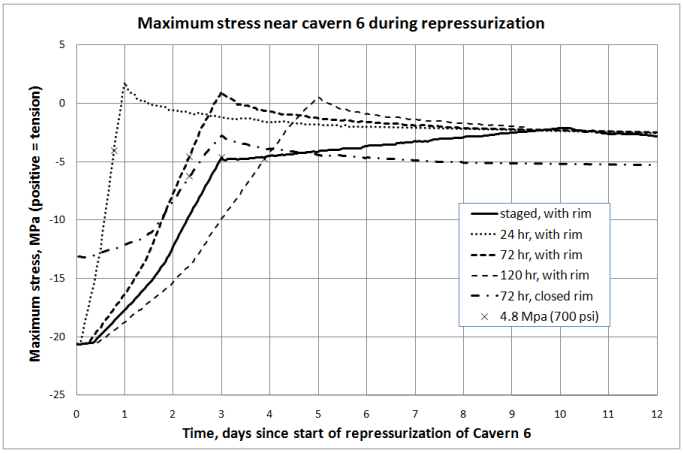

Figure 7. Maximum stress around Cavern 6 during repressurization

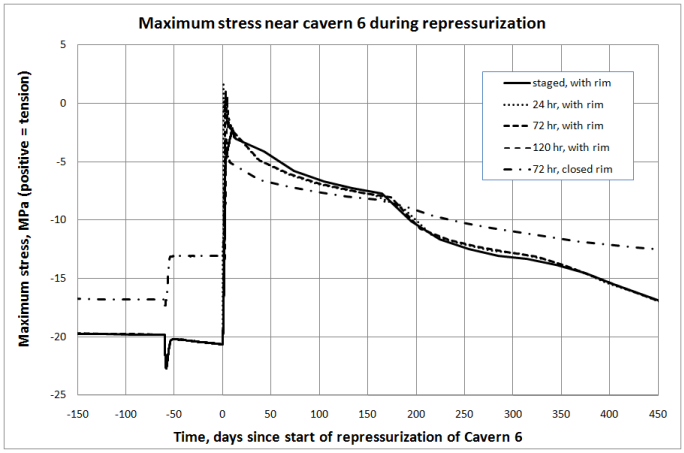

Figure 8. Maximum stress around Cavern 6 over a year after repressurization.

The damage factor used in this study is identified by a dilatant damage criteria defined by a linear function relating shear stress to hydrostatic pressure. Dilatancy is considered the onset of damage to rock resulting in significant increases in permeability. Dilatant damage in salt typically occurs at the point at which microfracturing initiates, resulting in volume increase. Dilatant criteria typically relate two stress invariants: the first invariant of the Cauchy stress tensor I_1 (equal to three times the mean stress) and the square root of the second invariant of stress deviator J_2, or $\sqrt{J_2}$ (a measure of the overall deviatoric or shear stress). One dilatant criterion is the linear equation typically used from Van Sambeek et al. (1993),

$$\sqrt{J_2} = 0.27 I_1 . \quad (1)$$

This damage criterion defines a linear relationship between I_1 and $\sqrt{J_2}$, and such linear relationships have been established from many suites of lab tests on WIPP, SPR, and other salt samples. This criterion was applied during post-processing of the analyses. A damage factor index was defined for this criterion (DF) by normalizing $\sqrt{J_2}$ from Equation 1 by $\sqrt{J_2}'$ yielding:

$$DF = \frac{0.27 I_1}{\sqrt{J_2}'} , \quad (2)$$

where J_2' is the value of the second invariant of the stress deviator tensor predicted from the simulation at every point in the mesh. Several earlier publications define that the linear damage factor DF indicates damage when DF=1, and failure when $DF \leq 0.6$. This report will use these damage thresholds.

The minimum safety factors typically occur during the workover periods, when the pressure at the wellhead is reduced to 0 MPa. When the minimum safety factor in the salt is plotted as a function of time, observations can be made regarding the change in safety factor as the initial cavern radius is increased, and as a function of time. Figure 9 shows the minimum value of dilatant damage factor obtained for each of the five simulations. A value of 1 indicates the onset of dilatant damage; typically, it is desired to keep the damage factor above 1.5. For the three cases with a rim and steady repressurization, the damage factor drops below 1, indicating the onset of damage. Fortunately, when the pressure increase ends, stress equilibration begins immediately and the damage factor rises back above 1 very quickly. For the case of no rim, the damage factor briefly drops below 1.5 at the maximum wellhead pressure, and then recovers. This result also differs from the result using the power law creep model, which predicted a damage factor below 1 for the same cavern geometry. For the case using staged repressurization, a minimum value of the damage factor of 1.34 is reached shortly after the maximum wellhead pressure is achieved at 10 days. This result demonstrates that at least seven days should be allowed to increase the wellhead pressure from 4.8 to 5.9 MPa.

The results presented here show that the pressure in Cavern 6 can be raised reasonably quickly to 4.8 MPa. This will help to minimize storage volume loss due to creep. Then a much slower pressure rise is warranted to prevent damage to the salt around the cavern. This repressurization process has not been violated by previous workovers for Cavern 6; Figure 10 shows historic repressurization data from previous workovers along with the current recommended limit to re-pressurize.

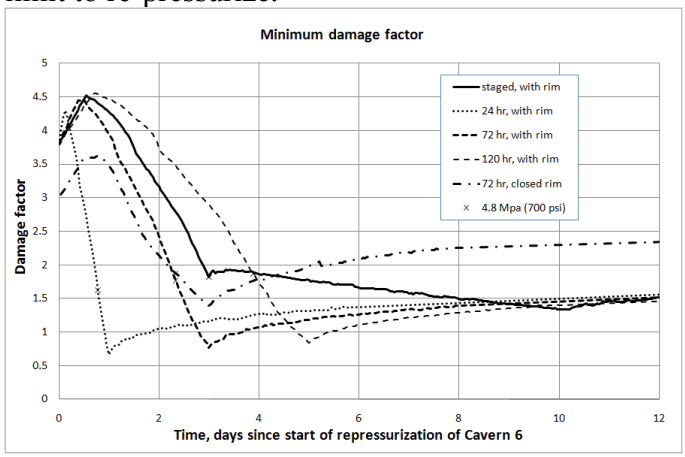

Figure 9. Minimum dilatant damage factor around Cavern 6 during repressurization.

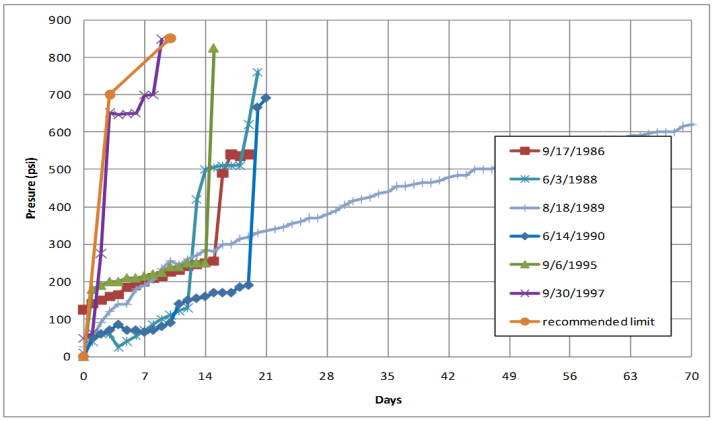

Figure 10. Re-pressurization histories following previous workovers of Cavern 6

As these calculations and others have shown, the primary causative mechanism of the well failures at SPR sites is subsidence induced by ground strains along the axis of the wellbore due to salt creep and cavern closure. These calculations also demonstrated that following a workover in Cavern 6, repressurization of the cavern must be performed slowly to avoid tensile fracturing at the roof. Based on these results, it was recommended to DOE that the wellhead pressure in Cavern 6 be re-pressurized to 4.8 MPa (700 psi) over three days, followed by an additional seven-day period (minimum; longer would be better) to raise the wellhead pressure to 5.9 MPa (850 psi). The initial and more rapid pressure increase would help mitigate creep closure losses in the cavern. The subsequent and more sensitive pressure rate must be slower to avoid tensile fracturing at the edge of the large flat diameter roof.

Following the completion of wellbore cementing on January 5, 2011, the repressurization of the cavern started on January 14, 2011 and lasted throughout January following the recommendations in this report. The wellhead pressure in Cavern 6 was raised to 4.8 MPa (700 psi) over three days, followed by an additional fourteen-day period to raise the wellhead pressure to the low end of its normal operating range, 5.9 MPa (850 psi) on January 31, 2011. Based on all indications from well pressure measurements from Caverns 6 and 9, there has been no event indicative of additional well damage or loss of cavern integrity since the workover was completed.

6 RESULTS OF ADDITIONAL ANALYSES FOR CAVERN 9

Following the well remediation in West Hackberry Cavern 6, additional concerns were raised about the potential effect of a similar procedure on Cavern 9. The initial analyses recommended that workovers performed on Caverns 9 should be performed no sooner than one year after the completion of a workover in Cavern 6. This period would allow the stressed salt around Cavern 6 enough time re-equilibrate and attain near-hydrostatic stress values, so to minimize the possibility of cracking the salt between Caverns 6 and 9, and reduce the possibility of damage under the ledge in Cavern 9 during its workover. The analyses reported in Sobolik and Ehgartner (2009) on West Hackberry, which used the power law creep model with a reduced elastic modulus, indicated that the ledge in Cavern 9 may achieve dilatant stress values during both ends of the workover process. The Cavern 6 calculations discussed above used the M-D model, which does not exaggerate transient response as using the reduced modulus does, and predicted a less severe (though still potentially tensile and dilatant) reaction to pressure changes for Cavern 6. To address additional concerns about the interactions between Caverns 6 and 9, two new sets of calculations were proposed: 1) A workover procedure on Cavern 9 that would begin three months after the completion of the recent Cavern 6 procedure; and 2) a workover of Caverns 6 and 9 simultaneously, also known as being operated as a gallery.

The workover simulation for Cavern 9 was restarted from the end of the Cavern 6 calculations with the staged repressurization, and utilized a similar cavern pressure history. The workover on Cavern 9 began on Day 107 after the beginning of Cavern 6 repressurization, with a five-day decrease from operating to zero wellhead pressure. On the 60th day of the workover (Day 167), the pressure was raised to 4.8 MPa (700 psi) over 3 days, then to 5.9 MPa (850 psi) over an additional 7 days (to Day 177), where it is held for another 8 days until raised to its original wellhead pressure of 6.38 MPa (925 psi).

Figure 11 shows the maximum principal stress around Caverns 6 and 9 from the beginning of the Cavern 6 workover (Day -60 in the plots), through the repressurization of Cavern 6 (beginning on Day 0), and through the workover on Cavern 9. The solid line shows the predicted stress on Cavern 6 from the earlier calculations, without a workover on Cavern 9, whereas the dashed line shows the stress around Cavern 6 with its actual repressurization schedule and a Cavern 9 workover. The maximum tensile stress around Cavern 6 occurs at the edge of the rim, and for Cavern 9 it is in the "ledge", the circular structure projecting into the middle of the cavern (see Figure 2). Two important observations can be made from Figure 11: first, that neither cavern experinces tensile stress during these operations; and second, that the workover on Cavern 9 actually helps the edge of Cavern 6 reach steady state stress more quickly.

Figure 12 shows the minimum damage factor around Caverns 6 and 9, using the same time scale and scenarios as did Figure 11. Cavern 6 reaches a minimum damage factor of 1.75 on Day 172,

corresponding to the end of depressurization down to 0 MPa wellhead pressure. Also, the workover on Cavern 9 seems to accelerate how quickly the edge of Cavern 6 returns to a steady-state, low-shear stress. Note the interesting behavior for Cavern 9 during repressurization (Days 167 to 177). This behavior is examined in greater detail in Figure 13. During the first three days of repressurization up to 4.8 MPa wellhead pressure, the minimum damage factor at first increases, but during the third day begins to decrease. It appears that somewhere around 3.4 MPa wellhead pressure, the cavern pressure passes some sort of equilibrium point, and the increasing pressure then begins to increase the local shear stresses. Without going through a series of simulations, it can probably be recommended that a similar staged approach to repressurizing Cavern 9 be implemented so as not to bring the ledge to dilatant stress values.

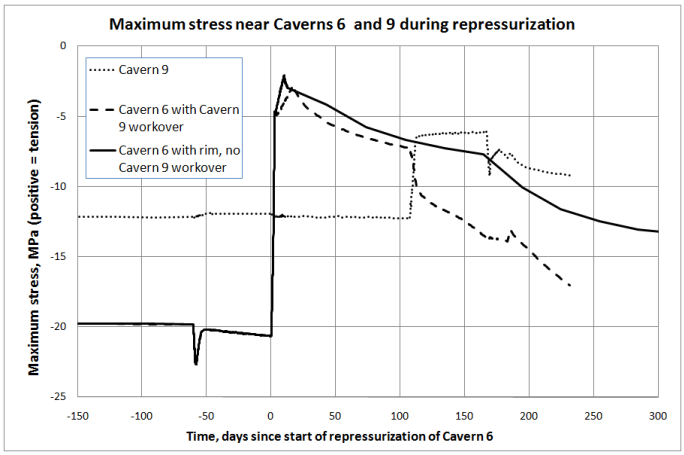

Figure 11. Maximum principal stresses near Caverns 6 and 9 during a workover on Cavern 9.

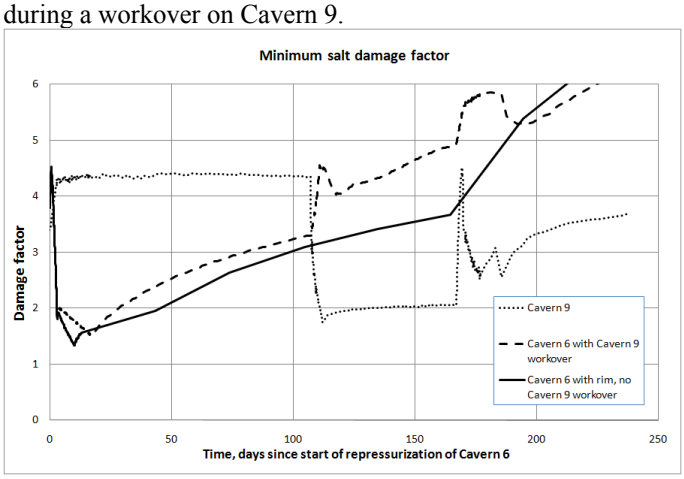

Figure 12. Minimum damage factor around Caverns 6 and 9 during a workover on Cavern 9.

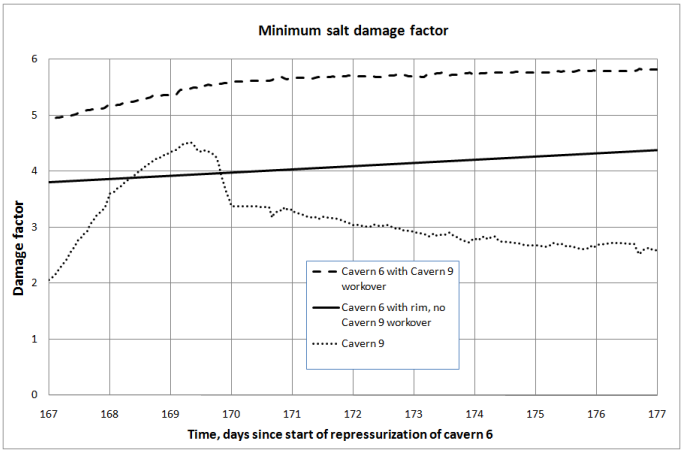

Figure 13. Expansion of Figure 12 to time of repressurization of Cavern 9.

The main conclusion from this set of calculations is that a workover on Cavern 9 may be performed, if necessary, shortly after a workover on Cavern 6 has been completed. There are still some potential issues with the ledge in Cavern 9, and also the proximity to Cavern 6, that require extra care during workover procedures. The calculations indicate that the repressurization of Cavern 9 after a workover should be done in done in a staged approach as was done for Cavern 6.

Because of the interaction between Caverns 6 and 9, the idea to operate the two caverns as a gallery has been proposed as a way to minimize the potential for crack initiation and propagation during a workover. A series of calculations was initiated that simulated performing a staged workover on both caverns simultaneously. Preliminary results indicated some potential concerns regarding shear stress at both ends of the workover cycle for both caverns. The analyses were not completed in time for inclusion in the paper, but results will be presented at a conference.

7 CONCLUSIONS

The computational model for the West Hackberry SPR site presented here is mature, with a mesh containing realistic geometries for the caverns and salt dome, a functional M-D model, and operating pressure scenarios that can be modified to fit current and new scenarios. Previous analyses with this model have been able to predict the well failures that occurred in the field, such as the well failure in Cavern 6. The first analysis presented in this report demonstrates the capability to apply complex, three-dimensional geomechanical computations to make recommendations to field operations in a short time frame. The recommended procedure insured a safe repressurization of Cavern 6, and there has been no event indicative of additional well damage or loss of cavern integrity since the workover was completed. The additional analyses in this report demonstrate the capability to anticipate potential problems that

may occur in the field, and plan operational procedures to prevent or mitigate negative consequences.

ACKNOWLEDGEMENT

Sandia National Laboratories is a multi-program laboratory operated and maintained by Sandia Corporation, a wholly owned subsidiary of Lockheed Martin Corporation, for the United States Department of Energy's National Nuclear Security Administration under Contract DE-AC04-94AL85000.

REFERENCES

Blanford, M.L., M.W. Heinstein, & S.W. Key, 2001. *JAS3D. A Multi-Strategy Iterative Code for Solid Mechanics Analysis. **User's Instructions**, Release 2.0.* SEACAS Library, JAS3D Manuals, Computational Solid Mechanics / Structural Dynamics, Sandia National Laboratories, Albuquerque, NM.

Munson, D.E. and P.R. Dawson, 1979. *Constitutive Model for the Low Temperature Creep of Salt (With Application to WIPP).* SAND79-1853, Sandia National Laboratories, Albuquerque, New Mexico.

Munson, D.E. and P.R. Dawson. 1982. *A Transient Creep Model for Salt during Stress Loading and Unloading.* SAND82-0962, Sandia National Laboratories, Albuquerque, New Mexico.

Munson, D.E. and P.R. Dawson, 1984. Salt Constitutive Modeling using Mechanism Maps. *I^st^ International Conference on the Mechanical Behavior of Salt, Trans Tech Publications*, 717-737, Clausthal, Germany.

Munson, D.E., 1998. *Analysis of Multistage and Other Creep Data for Domal Salts*, SAND98-2276, Sandia National Laboratories, Albuquerque, NM.

Munson, D.E., A.F. Fossum, and P.E. Senseny. 1989. *Advances in Resolution of Discrepancies between Predicted and Measured in Situ WIPP Room Closures.* SAND88-2948, Sandia National Laboratories, Albuquerque, New Mexico.

Munson, D.E., 2006. *Features of West Hackberry Salt Caverns and Internal Structure of the Salt Dome*, SAND2006-5409, Sandia National Laboratories, Albuquerque, New Mexico.

Rautman, C.A., J.S. Stein, and A.C. Snider, 2004. *Conversion of the West Hackberry Geological Site Characterization Report to a Three-Dimensional Model*, SAND2004-3981, Sandia National Laboratories, Albuquerque, New Mexico.

Sobolik, S.R. and B.L. Ehgartner, 2009. *Analysis of Cavern Stability at the West Hackberry SPR Site*. SAND2009-2194, Sandia National Laboratories, Albuquerque, New Mexico.

Sobolik, S.R., J.E. Bean, and B.L. Ehgartner, 2010. Application of the Multi-Mechanism Deformation Model for Three-Dimensional Simulations of Salt Behavior for the Strategic Petroleum Reserve, ARMA 10-403, 44th US Rock Mechanics Symposium and 5th U.S.-Canada Rock Mechanics Symposium, held in Salt Lake City, UT June 27–30, 2010.

Van Sambeek, L.L., J.L. Ratigan, & F.D. Hansen, 1993. *Dilatancy of Rock Salt in Laboratory Tests*, Int. J. Rock Mech. Min. Sci. & Geomech. Abstr. Vol. 30, No. 7, pp 735-738.

Whiting, G. H., 1980. *Strategic Petroleum Reserve (SPR): Geological Site Characterization Report, West Hackberry Salt Dome*, SAND80-7131, Sandia National Laboratories Albuquerque, New Mexico.